



Combustion characteristics of a micro segment platinum tubular reactor with a gap[☆]



Yu-Ting Wu^{a,c}, Yueh-Heng Li^{b,c,*}

^a Department of Engineering Science, National Cheng Kung University, Tainan 701, Taiwan, ROC

^b Department of Aeronautics and Astronautics, National Cheng Kung University, Tainan 701, Taiwan, ROC

^c Research Center for Energy Technology and Strategy, National Cheng Kung University, Tainan 701, Taiwan, ROC

HIGHLIGHTS

- Flame-anchoring mechanism of a micro-TPV reactor is numerically investigated.
- The gap on the platinum can provide a low-velocity region to stabilize micro flames.
- It allows to trade fuels and radicals from the inner and outer streams through gap.
- The catalytically induced combustion can be anchored on the micro-TPV reactor.

ARTICLE INFO

Article history:

Received 22 March 2016
Received in revised form 19 June 2016
Accepted 22 June 2016
Available online 23 June 2016

Keywords:

Catalytic combustion
Platinum
Small-scale reactor
Heterogeneous and homogenous reaction
Thermophotovoltaic

ABSTRACT

The present study proposes a conceptual design for a combustion chamber for overcoming critical heat loss and flame instability in a micro-thermophotovoltaic power system (micro-TPV). In the design, a platinum tube is used simultaneously as a catalyst reactor and an emitter. The flame-stabilizing mechanisms of a TPV reactor are numerically investigated regarding the effects of reactor configuration and fuel concentration. The interaction of heterogeneous and homogeneous reactions between the inner and outer chamber of the TPV reactor is also examined. Results indicate that the catalytically induced combustion can be anchored in the gap between two segmented platinum tubes by inheriting thermal energy and radicals from the upstream section of the segmented catalyst. The gap not only provides a low-velocity region for stabilizing flames, but also enables the exchange of fuels and radicals from the inner and outer streams.

© 2016 Elsevier B.V. All rights reserved.

1. Introduction

With the rapid progress in electromechanical and electrical consumer devices such as laptop computers, mobile phones, and aerial drones in recent years, the demands on micro power sources with high power densities are increasing. Characteristically, required power densities range from 10 to 1000 W/kg and energy densities from 500 to 5000 Wh/kg [1]. State-of-the-art battery technology (e.g., Li-ion batteries) is unable to deliver the levels of power and energy densities required for future portable electronic

and electromechanical applications. In addition, batteries have a considerable environmental impact, high cost, and long recharging time. An alternative is the utilization of hydrocarbon fuels in combustion-driven micro-scale power sources. A number of notable theoretical and experimental works have exemplified and demonstrated the benefits of scaled-down power generating devices involving combustion-driven thermal cycles with the use of internal micro-combustion engines, micro gas turbine engines, and micro piezoelectric devices. Because of substantial technical difficulties in maintaining structural integrity and minimizing heat dissipation through the various system components, the development of micro thermophotovoltaic (micro-TPV) devices has drawn attention to capitalize on direct energy conversion without moving parts [2]. Therefore, thermophotovoltaics utilize photovoltaic cells to generate electricity from the radiation of a high-temperature source. TPV conversion employs a variety of heat sources that heat an emitter to a typically incandescent temperature to provide radiation. For providing a stable and controllable heat source in a TPV

[☆] This paper is submitted for publication in Chemical Engineering Journal. Material in this manuscript has neither been published in nor submitted to a journal previously, nor will it be submitted to another journal during the Chemical Engineering Journal review process.

* Corresponding author at: Department of Aeronautics and Astronautics, National Cheng Kung Univ., Tainan 701, Taiwan, ROC.

E-mail address: yueheng@mail.ncku.edu.tw (Y.-H. Li).

power system, burning fossil fuel is a straightforward and reliable approach with the benefits of inherently high energy density, immediate use, and ease of supply.

In miniaturization processes, the increasing surface-to-volume ratio of a micro-TPV reactor causes difficulty in maintaining the heat generated from the combustion process because of the heat loss to the wall, and concurrently enhances the possibility of radical termination through wall reactions. Consequently, a major challenge in the design of micro-TPV reactors is maintaining sustainable combustion and maximizing radiation heat output from the TPV emitter. To overcome these challenges, stabilization of flames in a micro-TPV system can be achieved through several methods. The most common method is to use simple configurations such as a backward-facing step, a bluff-body, or a cavity to induce flow recirculation and stabilize flames in a confined chamber. Wan et al. [3] employed a cavity in a micro combustor to generate a recirculation zone and stabilize flames in the cavity. Yang et al. [4] and Yadav et al. [5] used a backward facing step to anchor flames inside the micro reactor. In addition, a porous inert medium (PIM) is employed in a micro-TPV combustor to enhance the heat transfer capability between high-temperature combustion products and the combustor wall by capitalizing on the high thermal conductivity and emissivity of the solid matrix. PIM micro-combustion can yield high power density and increase the power and operational range of lean flammability. Yang et al. [6] and Chou et al. [7] have used SiC porous medium foam employed in a micro modular combustor to augment the combustion stability and radiation uniformity of an emitter. Alternatively, catalytic combustion is a plausible solution for overcoming the challenges associated with increasing surface-to-volume ratios. Platinum is also considered a selective material for delivering the radiation congregated in a short wavelength spectrum, and it is advantageous for maximizing the overlapping area between the radiant spectrum of the emitter and the bandgap range of PV cells. Therefore, catalytic materials are engaged on the micro-reactor walls to reduce the impact of thermal quenching [8,9]. Li et al. [10,11] have demonstrated that the deployment of catalyst segmentation and a cavity in a micro-channel can significantly stabilize catalytically-induced combustion in the reactor. The heterogeneous reaction in a prior catalyst segment produces chemical radicals and catalytically induced exothermicity, and the homogeneous reaction can be subsequently ignited and anchored in the following cavity. The concept of micro-channel design was adopted to design a tubular platinum reactor with perforated holes was fabricated and assessed with hydrogen fuel, and the corresponding combustion behaviors and operational ranges were subsequently examined [12].

Except for the radiation from an emitter, flames are regarded as an alternative radiation source to be further collected and converted into electricity through photovoltaic cells. It is feasible to manipulate the intensity of flame radiation by adjusting the fuel composition of gas mixtures [13] or by adding various volumetric concentrations of iron pentacarbonyl into liquid hydrocarbon fuels [14]. Unlike the flames confined in the combustion chamber and expected to heat only the emitter, Li et al. [13,14] have used high-luminescent flames to encompass and heat the emitter in a micro-TPV system. The results demonstrated a significant increase in the radiation efficiency of the TPV system engendered by the simultaneous collection of radiation from flames and the emitter.

The aim of the present study was to improve the radiation intensity of micro-TPV reactors by simultaneously converting radiation from flames and an emitter into electricity. The corresponding high surface-to-volume ratios at the microscale engender flame stabilization difficulty because of thermal and radical quenching on the combustor walls. Accordingly, the concept of micro-TPV combustor design originates from the aforementioned flame stabi-

lization mechanism of the micro-channel with catalyst segmentation and cavities [10,11] and the heat recirculation mechanism of Swiss-roll combustors [15]. The configuration of the proposed micro-TPV combustor comprises two platinum tube segments with a gap. The gap has a function similar to a cavity for decelerating the flow in localized spaces, as well as a channel to trade and collect the fuel and radicals from two sides. The distribution of different equivalence ratios of fuel–air mixtures through the inner and outer chamber of the reactor is a deliberate strategy for sustaining maximal incandescence over platinum tubes with minimal fuel consumption. The catalytically-induced flames are anticipated to be stably anchored on the outer surface of the reactor, and the purpose of radiation integration is achieved in the design of the segmented TPV reactor. Therefore, this study numerically investigated the functionality of a gap between the segmented catalytic tube in terms of flame stabilization and combustion behaviors.

2. Numerical method

To demonstrate and validate the aforementioned concept that is feasible in a micro-TPV combustor, a numerical simulation was performed with a commercial CFD-ACE + program [16]. Fig. 1 shows the schematic configuration of the proposed micro-TPV combustor that consists of two platinum tube segments with a gap of 1 mm. The dimensions of the two platinum tube segments are 5.3 mm (ID) \times 6 mm (OD) \times 4.5 mm (L) and 5.3 mm (ID) \times 6 mm (OD) \times 44.5 mm (L), respectively. The platinum tubes are coaxially placed in a quartz tube with a dimension of 8 mm (ID) \times 10 mm (OD) \times 50 mm (L), and this coaxial reactor constitutes the central (inner) and annulus (outer) chambers. The cross sections in the central and the annulus are approximately identical. In this study, different equivalence ratios of H₂–air mixtures were individually introduced to the inner and outer chamber of the TPV reactor. The inlet temperature was 300 K and a uniform velocity profile (20 m/s) was specified at the inlet. At the exit, a constant ambient pressure of 101 kPa was specified, and an extrapolation scheme was used for species and temperature. Chemical reaction mechanisms are used in the gas phase as well as on the catalyst surface. The homogeneous reaction mechanism proposed by Miller and Bowman [17] was used for hydrogen–air combustion, and this mechanism comprises of 9 species and 19 reaction steps. The surface reaction mechanism was compiled primarily from that proposed by Deutschmann et al. [18]. These reaction mechanisms have been used in previous studies [19] and the comparisons with experimental results are satisfactory [20]. In this study, the effects of reactor configuration, fuel concentration, and flow velocity on the flame stabilization mechanism were addressed and discussed. This study emphasizes the thermal and chemical effects in the vicinity of the gap between the catalyst segments, not the optimization of reactor dimension.

3. Results and discussion

3.1. Effect of reactor configuration

Regarding the effect of reactor configuration, two identical platinum reactors, plain and segmented platinum tubes with a gap, were employed to investigate the effects of the reactor configuration and fuel–air distribution on the performance of the micro-TPV reactor. Fig. 2 shows the local distributions of OH mass fractions overlaid with velocity vectors and local equivalence ratio (LER) level lines for the two catalyst configurations at a fixed inlet velocity of 20 m/s in the inner and outer chambers. The upper panel of Fig. 2 shows the numerical results for the segment

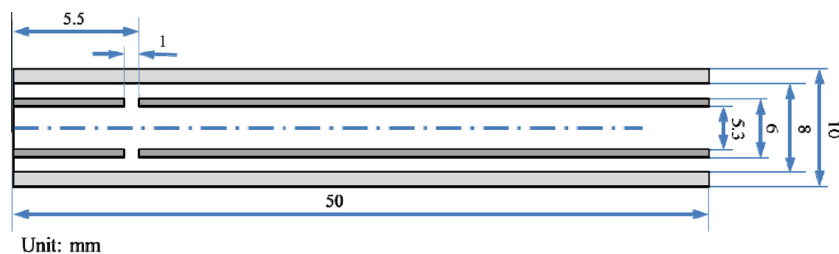


Fig. 1. Schematic of the segmented platinum reactor with a gap.

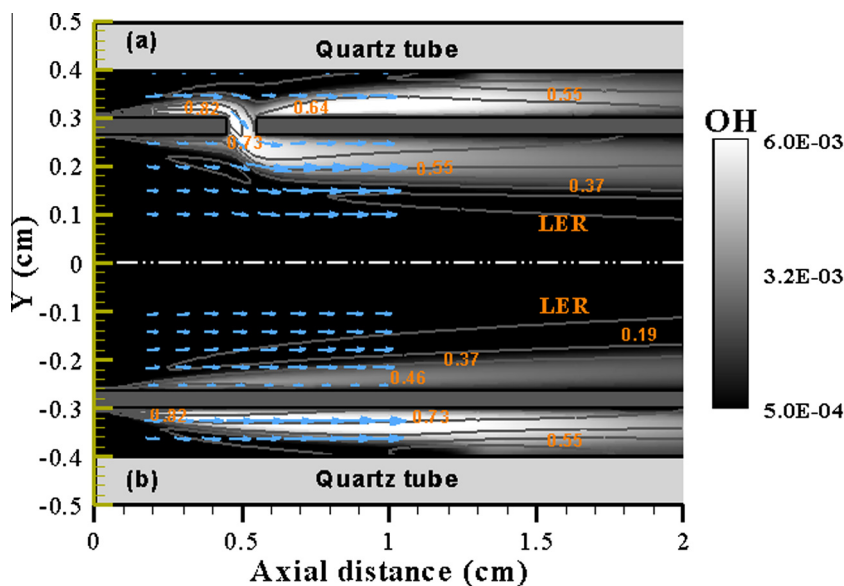


Fig. 2. Distributions of OH mass fractions overlaid with velocity vectors and LER level lines for the two catalyst configurations, (a) segmented platinum and (b) plain platinum reactors, respectively, at a fixed inlet velocity of 20 m/s in the inner and outer chambers.

platinum tubes with a gap, and the lower panel displays the plain platinum tube. The equivalence ratio of the hydrogen–air mixture was 0.3 for the inner chamber and 0.6 for the outer chamber. The definition of an LER is based on the local balance of hydrogen and oxygen atoms of eight major species (H_2 , O_2 , H , O , OH , HO_2 , H_2O , and H_2O) involved in H_2 and O_2 reactions [3], as given by Eq. (1).

$$LER = \frac{\frac{1}{2} \times (X_{H_2} + X_{H_2O} + X_{H_2O_2}) + \frac{1}{4} \times (X_H + X_{OH} + X_{HO_2})}{\frac{1}{2} \times (X_O + X_{H_2O} + X_{OH}) + X_{O_2} + X_{HO_2} + X_{H_2O_2}} \quad (1)$$

Concerning the plain platinum tube, hydrogen at the inner surface of the platinum tube was initially reacted heterogeneously and provided catalytically-induced exothermicity to facilitate hydrogen conversion on the outer surface through thermal conduction on the tube. The distribution of the computed OH mass fraction presents the flame location. The flame was typically anchored in the low-velocity region of the boundary layer along the outer surface. The relationship between the inner and outer chambers is associated only with the heat transfer interaction on the platinum tube. Regarding the segmented platinum tube, the distribution of velocity vectors implies the interaction of fluid dynamics between the inner and outer chambers; the mixtures in the outer chamber appear to flow toward the inner chamber. Accordingly, the LERs in the vicinity of the gap were incremental. According to the distribution of the computed OH mass fraction, abundant OH radicals generated on the outer surface of the upstream section of the segmented platinum tube were noted to induce the sequential homogeneous reactions over the inner and

outer surfaces of the downstream section of the segmented tube. Specifically, the catalytically-induced homogeneous reaction could stabilize in the gap by inheriting thermal energy and radicals from the upstream section of the segmented catalyst. The interactions between the inner and outer chambers are complicated—they involve the influences of flow behavior, mass diffusion of the mixture, and the heat transfer effect.

Fig. 3 shows the ratio of surface mass fraction (Y_s) to mean bulk mass fraction (Y_b) along the inner and outer surfaces of the platinum tubes. In general, a heterogeneous reaction is considered to be kinetically controlled, in which the surface concentration is greater than 95% of the bulk concentration, and mass transfer controlled, in which the surface concentration is less than 5% of the bulk [10]. No significant difference existed regarding the distribution of hydrogen mass fraction between the two configurations because hydrogen has inherently large mass diffusivity and a high sticking coefficient to platinum catalysts. Bumps were observed in the fuel mass fraction along the inner and outer surfaces of the segmented platinum reactor, as shown in Fig. 3b. This is due to H_2 mass transfer occurring in the gap. Despite the effect of H_2 mass transfer, the heterogeneous reaction of the two configurations was regarded as a mass-transfer-controlled when the distance reached 0.4 cm.

Fig. 4 shows the H_2 and OH radial mass fraction and temperature distribution along the axial direction near to the inner and outer surfaces of the two platinum reactors in the first 2-cm span from the inlet. The numerical results demonstrated that complete consumption of hydrogen was achieved within the 2-cm-long

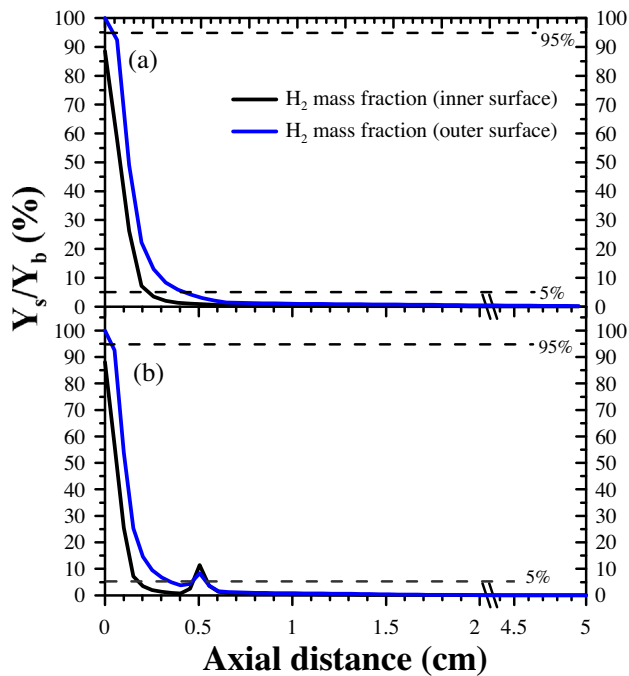


Fig. 3. Fuel mass fraction along the inner and outer surfaces of the (a) plain platinum and (b) segmented platinum reactors.

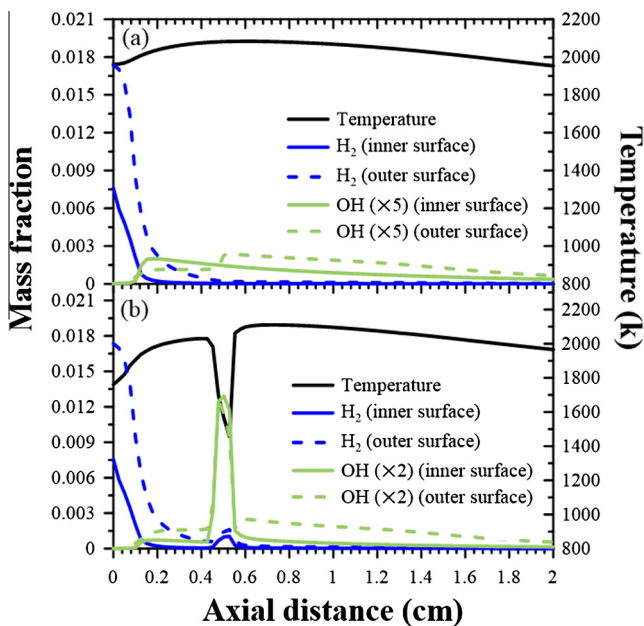


Fig. 4. H₂ and OH radial mass fractions and temperature distributions along the axial direction near the inner and outer surfaces of the (a) plain platinum and (b) segmented platinum reactors in the first 2-cm span from the inlet.

catalyst tube in both configurations. For the plain platinum reactor, H₂ was prone to light off early on both sides of the platinum tube because of its high mass diffusivity, as shown in Fig. 4a. No significant difference was observed regarding the inception of the OH mass fraction in the vicinity of the inner and outer surfaces. However, for the segmented platinum reactor, bumps in H₂ concentration distributions appear in the location of the gap, where H₂ exhibited no heterogeneous consumption but exhibited concentration accumulation because of mass transfer from mean stream. The drop in

temperature distribution was caused by the dilution of the low-temperature mixtures in the gap, whereas the OH radical concentration abruptly rose in the gap, indicating the occurrence of a homogeneous reaction.

Figs. 5 and 6 demonstrate the H and OH mass fractions and temperature distribution along the axial direction near the inner and outer surfaces of the two platinum reactors in the first 2-cm span from the inlet. The presence of gaseous species, H and OH, denoted the occurrence of a gas reaction, whereas the presence of surface species, H(*) and OH(*), implies the occurrence of a surface reaction. The concentrations of the H and OH radicals in the plain platinum tube were approximately an order of magnitude lower than those in the segmented platinum tube, but the concentrations of the H(*) and OH(*) surface radicals were similar in both configurations. The mass diffusivity and sticking coefficient of H₂ were inherently higher than those of O₂; therefore, the distribution of surface species concentration over the inner surface of the platinum tube was dominated by increasing H(*) and followed by increasing OH(*). Compared with the results in Fig. 3, the distribution of H(*) coincided with the distribution of the H₂ mass fraction ratio, the value of which was higher than or equal to 5%. After the dominant H₂ diffusion zone, O₂ was subsequently diffused to the catalyst surface and yielded the surface radical OH(*). As opposed to the absence of a significant increase in gaseous radical concentrations over the inner surface of the plain platinum tube, H and OH radical concentrations apparently increase in the vicinity of the gap for the segmented platinum tube. The surface reaction occurring in the upstream section of the segmented platinum tube was expected to sequentially assist the inception of the gas reaction in the downstream section of the tube. Consequently, gas and surface reactions were sustained in the inner chamber of the segmented platinum tube, whereas only a surface reaction occurs on the inner surface of the plain platinum tube. Conversely, because of the increasing hydrogen concentration, the concentrations of gaseous and surface species evidently increased over the outer surface of the plain platinum tube, as seen in Fig. 6a. This implies the occurrence of catalytic combustion. Typically, a radical

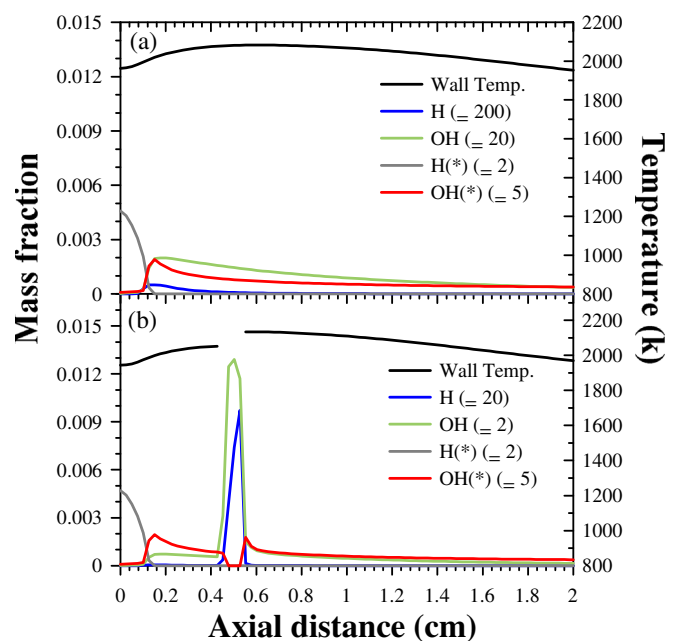


Fig. 5. H and OH mass fractions and temperature distributions along the axial direction near the inner surface of the (a) plain platinum and (b) segmented platinum reactors in the first 2-cm span from the inlet.

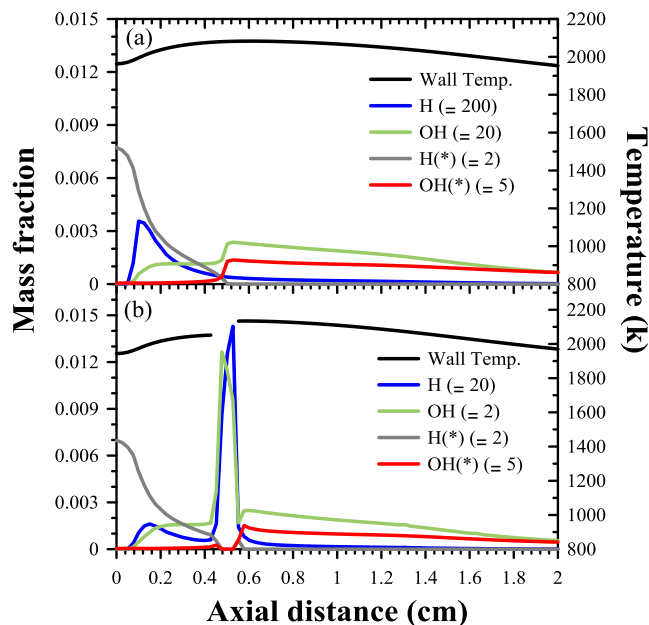


Fig. 6. H and OH mass fractions and temperature distributions along the axial direction near the outer surfaces of the (a) plain platinum and (b) segmented platinum reactors in the first 2-cm span from the inlet.

competition exists between gas (homogeneous) and surface (heterogeneous) reactions over plain platinum, which leads to low concentrations in gaseous species. The coexistence of gas and surface reactions was observed on the outer surface of the segmented platinum tube (Fig. 6b). The significant difference between the results in Figs. 5b and 6b is the concentration distribution of the H radical along the upstream section of the segmented platinum tube and the gap. The H radical concentration around the upstream section of the segmented catalyst and the gap in the outer chamber was higher than that in the inner chamber. In principle, the hydrogen concentration in the outer chamber is richer than that in the inner chamber, and the abundant and unburnt hydrogen travels from the outer chamber to the inner chamber through the gap. Tracking the chemical reactions of hydrogen combustion along the outer surface of the segmented platinum tube indicated that the chemical reaction rate of R1 ($\text{OH} + \text{H}_2 = \text{H}_2\text{O} + \text{H}$) was predominantly higher than the reverse chemical reaction rate of R2 ($\text{O} + \text{OH} = \text{O}_2 + \text{H}$). Specifically, the production rate of the H radical was somehow higher than the consumption rate of the H radical. By contrast, the chemical reaction rate of R1 apparently decreased to a certain magnitude equivalent to that of R3 ($\text{H} + \text{HO}_2 = 2\text{OH}$), and R3 replaced the importance of R2 along the inner surface of the segment platinum tube. Ultimately, this resulted in a reduction in the H radical concentration in the gap of the inner chamber.

Regarding the plain platinum tube, the heterogeneous reaction was sustained in the inner chamber, whereas the hetero- and homogeneous reactions were sustained in the outer chamber because of their relatively high equivalence ratios. The interaction between the inner and outer chambers was associated with the heat transfer on the platinum tube. Regarding the segmented platinum tube, however, the gap played an essential role in microflame stabilization by providing a low-velocity region, a heat source, and significant amounts of chemical radicals such as H, O, and OH. The gap increased the aerodynamic and chemical effects in both chambers, despite the dominant chemical reaction steps of gas reaction being different, resulting in various H radical concentrations.

3.2. The effect of fuel concentration

To understand the effect of fuel concentration, equivalent fuel–air mixtures were introduced to the inner and outer chambers to diminish the influence of mass diffusion driven by the concentration gradient. Accordingly, two fuel deployments were realized: $\text{ER}_{\text{in}} = 0.3/\text{ER}_{\text{out}} = 0.6$, and $\text{ER}_{\text{in}} = \text{ER}_{\text{out}} = 0.45$, both of which were engaged in the segmented platinum reactor with identical total hydrogen inputs. Fig. 7 demonstrates the distribution of the OH mass fraction overlaid with velocity vectors and LER level lines for the different fuel concentrations. According to the OH radical distribution, the flame sustained in the gap and tailed only toward the inner and outer chambers (Fig. 7a). For $\text{ER}_{\text{in}} = \text{ER}_{\text{out}} = 0.45$, the flame sustained in the gap and tailed only toward the inner chamber (Fig. 7b). Remarkably, a flame was detached and anchored in the boundary layer on the outer surface downstream section of the segmented platinum tube. The velocity vectors demonstrate that the fluids flowed from the outer chamber toward the inner chamber through the gap, and the LER contours reveal the flammability of the gas mixture in the gap. Fig. 8 shows the temperature distribution overlaid with velocity vectors and velocity magnitude lines in the first 1-cm span from the inlet. Notably, the numerical results of the temperature and flow velocity in the gap and inner chamber shown in Fig. 8a are significantly higher than those shown in Fig. 8b. In general, higher flow velocities in the gap were associated with increasing hydrogen concentrations, specifically, a relatively large LER distribution occurred in the gap and along the downstream region of the catalyst surfaces, as shown in Fig. 7a. This induced the catalytic combustion sustained on the downstream section of the segmented platinum tube and generated a greater wall temperature and gas temperature distribution along the inner surface of the downstream section of the segmented platinum tube (Fig. 8a). This is in stark contrast to the wall temperature and gas temperature distribution along the inner surface in Fig. 8b. Accordingly, the flow velocities near to the inner surface of the downstream section of the segmented platinum tube were increased in the high-temperature regime, and this is associated with the increase in the flow velocities in the gap.

Fig. 9 shows fuel mass fraction along the inner and outer surfaces of the segmented platinum reactor for the two fuel deployments. Interestingly, the hydrogen mass fraction along the outer surface exhibited a larger bump in the location of the gap for $\text{ER}_{\text{in}} = \text{ER}_{\text{out}} = 0.45$. This proves that the flame in the outer chamber does not anchor in the gap, but instead on the outer surface

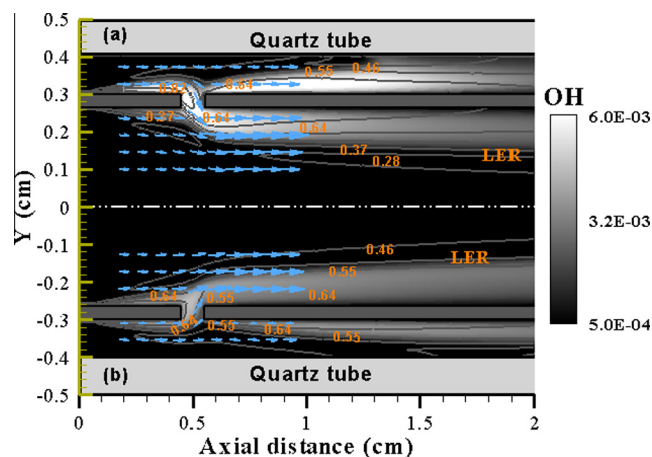


Fig. 7. Distributions of OH mass fractions overlaid with velocity vectors and LER level lines for (a) $\text{ER}_{\text{in}} = 0.3/\text{ER}_{\text{out}} = 0.6$, and (b) $\text{ER}_{\text{in}} = \text{ER}_{\text{out}} = 0.45$, respectively, at a fixed inlet velocity of 20 m/s in the first 2-cm span from the inlet.

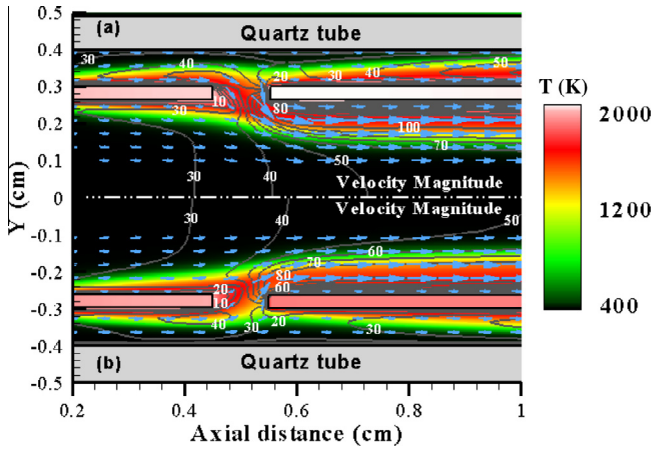


Fig. 8. Distributions of temperature overlaid with velocity vectors and LER level lines for (a) $ER_{in} = 0.3/ER_{out} = 0.6$, and (b) $ER_{in} = ER_{out} = 0.45$, respectively, at a fixed inlet velocity of 20 m/s in the first 1-cm span from the inlet.

because of the massive hydrogen flow from the inner chamber to the outer chamber. Otherwise, the heterogeneous reaction of the two configurations is regarded as a mass-transfer-controlled reaction. Fig. 10 shows the H_2 and OH radial mass fraction and temperature distribution along the axial direction near the inner and outer surfaces of the segmented platinum reactor in the first 2-cm span from the inlet. The gas temperature along the outer surface in Fig. 10a was higher in the upstream section of the segmented platinum tube but lower in the downstream section of this tube (Fig. 10b). This is because that the increase in the equivalence ratio in the inner chamber enhanced the chemical reaction along the upstream inner surface, leading to an enhanced gas reaction in the outer chamber because of the increasing wall temperature.

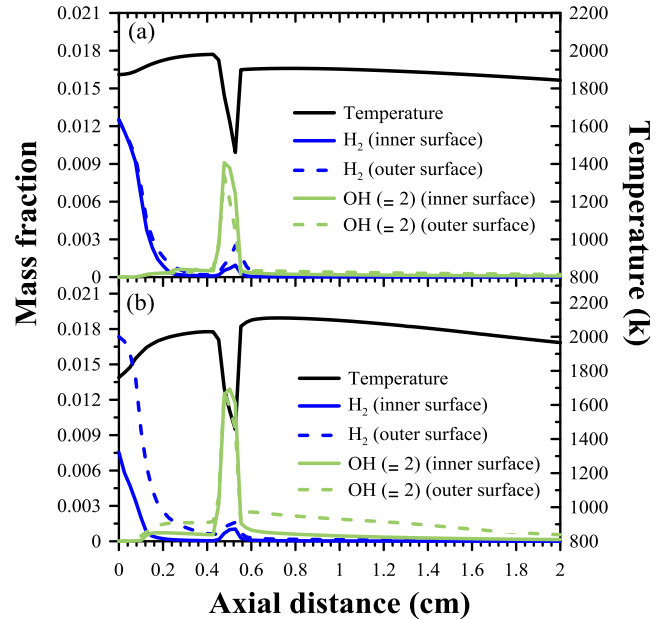


Fig. 10. H_2 and OH radial mass fractions and temperature distributions along the axial direction near the inner and outer surfaces of the segmented platinum reactor in the first 2-cm span from the inlet for (a) $ER_{in} = ER_{out} = 0.45$, and (b) $ER_{in} = 0.3/ER_{out} = 0.6$.

Nonetheless, the discontinuity of the flame and entrainment of fresh hydrogen in the gap of the outer chamber influenced the deterioration of the gas reaction and reduced the OH radical concentration. This explains the lower OH mass fractions shown in Fig. 10a compared with those shown in Fig. 10b. Furthermore, the hydrogen concentration was relatively low, resulting in the

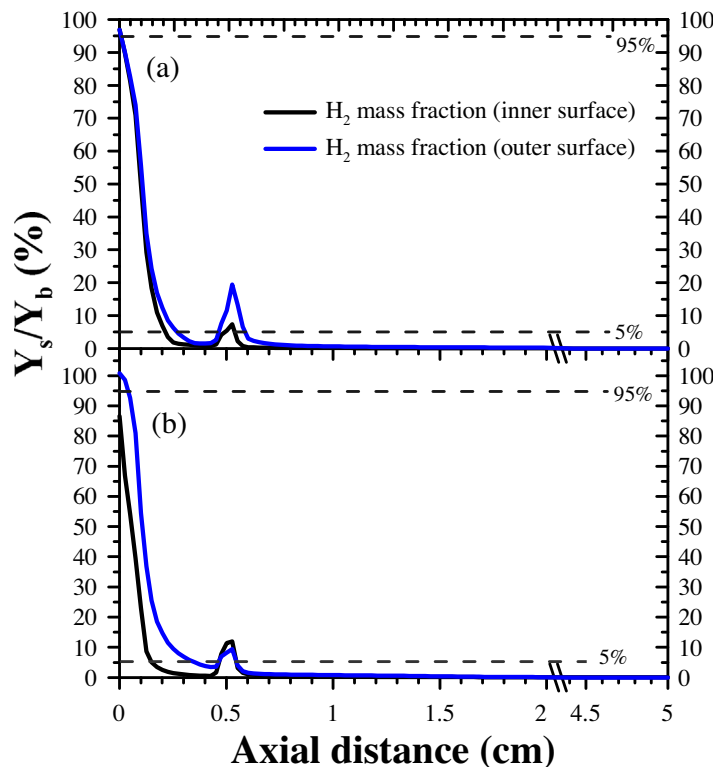


Fig. 9. Fuel mass fractions along the inner and outer surfaces of the segmented platinum reactor for (a) $ER_{in} = ER_{out} = 0.45$, and (b) $ER_{in} = 0.3/ER_{out} = 0.6$.

reduced gas temperature distribution along the outer surface on the downstream section of the segmented platinum tube, as shown in Fig. 10a and b.

Figs. 11 and 12 display the H and OH mass fractions and temperature distribution along the axial direction near the inner and outer surface of the segmented platinum reactor in the first 2-cm span from the inlet for the two fuel deployments. Because of the relatively high H_2 concentration shown in Fig. 11a, the $H(^*)$ concentration over the inner surface of the upstream section of the segmented platinum tube is apparently higher than that shown in Fig. 11b. Furthermore, the distribution of the $H(^*)$ mass fraction shown in Fig. 11a is wider than that shown in Fig. 11b. When $ER_{in} = ER_{out} = 0.45$, the hydrogen mass fraction ratio along the inner surface dropped to 5% when the axial distance reached 0.2 cm (Fig. 9a). However, for $ER_{in} = 0.3/ER_{out} = 0.6$, it dropped to 5% when the axial distance reached 0.15 cm. The $H(^*)$ radical distributions are consistent with the H_2 distribution in which the mass fraction ratio was higher than or equal to 5%. In addition, the OH mass fraction shown in Fig. 11 indicates that the inception of the homogeneous reaction occurred on the inner surface of the upstream section of the segmented platinum tube. Fig. 12a shows the $H(^*)$ mass fraction distribution on the outer surface of the upstream and downstream sections of the segmented platinum tubes. In particular, the pump of the $H(^*)$ mass fraction on the leading edge of the downstream section of the segmented platinum tube revealed the presence of a surface reaction and evident hydrogen entrainment from the main stream of the outer chamber to the inner chamber. Fig. 12b shows the $H(^*)$ mass fraction distribution over the outer surface of the upstream section of the segmented platinum tube according to the higher hydrogen mass fraction ratio, and the $OH(^*)$ mass fraction distribution was postponed to the downstream section of the segmented platinum tube. However, the H and OH radical concentrations were evidently increased on the outer surface of the upstream section of the segmented platinum tube when $ER_{in} = 0.3/ER_{out} = 0.6$. This implies that the flame anchored on the outer surface of the upstream segment platinum tube with the assistance of abundant radicals and thermal energy.

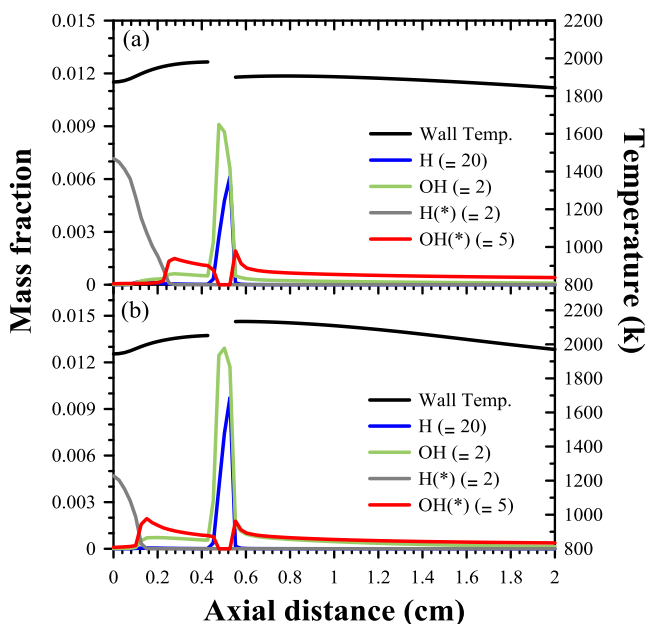


Fig. 11. H and OH radial mass fractions and temperature distributions along the axial direction near the inner surface of the segmented platinum reactor in the first 2-cm span from the inlet for (a) $ER_{in} = ER_{out} = 0.45$, and (b) $ER_{in} = 0.3/ER_{out} = 0.6$.

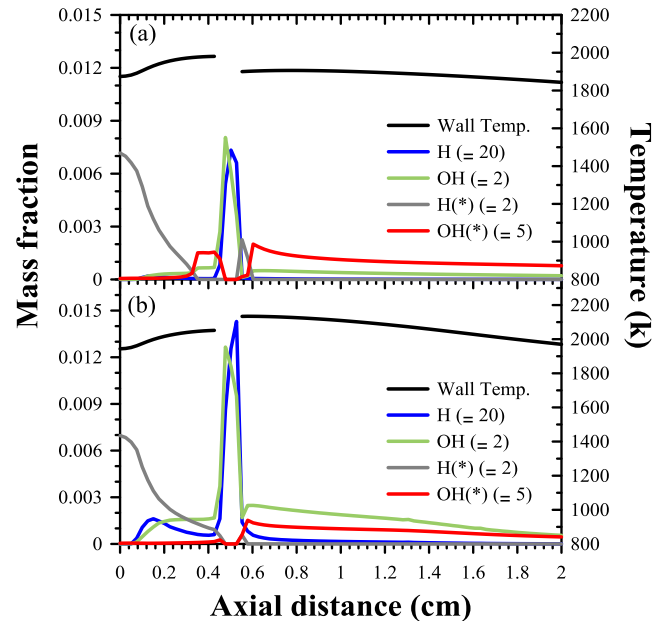


Fig. 12. H and OH radial mass fractions and temperature distributions along the axial direction near the outer surface of the segmented platinum reactor in the first 2-cm span from the inlet for (a) $ER_{in} = ER_{out} = 0.45$, and (b) $ER_{in} = 0.3/ER_{out} = 0.6$.

4. Conclusion

This study numerically discusses the flame-anchoring mechanism of a micro-TPV reactor in terms of the effects of reactor configuration and fuel concentration. The interaction between the inner and outer chambers is investigated according to the effect of aerodynamics, mass and heat transfer, and chemical reactivity. The following conclusions are obtained from this study.

1. The effect of reactor configuration in the plain platinum reactor and the segmented platinum reactor are discussed. In the plain platinum tube, flames are sustained in the boundary layer on the outer surface. The flame-stabilizing mechanism between the inner and outer chambers is associated with heat transfer interaction on the platinum tube. In the segmented platinum tube, the catalytically induced homogeneous reaction can stabilize in the gap by inheriting thermal energy and radicals from the upstream section of the segmented catalyst. The gap could provide a low-velocity region, heat source, and considerable amounts of chemical radicals such as H, O, and OH, which can facilitate micro combustion stabilization.
2. For the different fuel deployments, the flame is sustained in the gap and only tails toward the inner chamber when $ER_{in} = ER_{out} = 0.45$. On the outer surface of the downstream section of the segmented platinum tube, a flame is detached and anchored on the boundary layer. This is because an increase in the equivalence ratio in the inner chamber enhances the chemical reaction along the upstream inner surface, leading to an enhanced gas reaction in the outer chamber because of the increasing wall temperature. Nonetheless, the discontinuity of the flame and entrainment of fresh hydrogen in the gap of the outer chamber influence the deterioration of the gas reaction and reduce OH radical concentration. Therefore, appropriate fuel concentration in the inner chamber is a key parameter for sustaining a gas reaction anchored on the gap and fulfills the purpose of radiation integration from flames and the emitter.

Acknowledgements

This research was partially supported by the Ministry of Science and Technology (Republic of China, Taiwan) under Grant numbers MOST 104-2218-E-006-012 (Y.H. Li), MOST 104-2221-E-006-136 (Y.H. Li), and MOST 104-2111-M-006-001 (Y.T. Wu). Computer time and numerical packages provided by the National Center for High-Performance Computing, Taiwan (NCHC Taiwan), are gratefully acknowledged.

References

- [1] D. Dunn-Rankin, E.M. Leal, D.C. Walther, Personal power systems, *Prog. Energy Combust. Sci.* 31 (2005) 422–465.
- [2] H. Daneshvar, R. Pronja, N.P. Kherani, Thermophotovoltaics: Fundamentals, challenges, and prospects, *Appl. Energy* 159 (2015) 560–575.
- [3] J. Wan, A. Fan, H.Y. Liu, Flame-anchoring mechanisms of a micro cavity-combustor for premixed H₂/air flame, *Chem. Eng. J.* 275 (2015) 17–26.
- [4] W.M. Yang, S.K. Chou, C. Shu, Z.W. Li, H. Xue, Combustion in micro-cylindrical combustors with and without a backward facing step, *Appl. Therm. Eng.* 22 (2002) 1777–1787.
- [5] S. Yadav, P. Yamasani, S. Kumar, Experimental studies on a micro power generator using thermos-electric modules mounted on a micro-combustor, *Energy Convers. Manage.* 99 (2015) 1–7.
- [6] W.M. Yang, S.K. Chou, K.J. Chua, J. Li, X. Zhao, Research on modular micro combustor-radiator with and without porous media, *Chem. Eng. J.* 168 (2011) 799–802.
- [7] S.K. Chou, W.M. Yang, J. Li, Z.W. Li, Porous media combustion for micro thermophotovoltaic system applications, *Appl. Energy* 87 (2010) 2862–2867.
- [8] W.C. Pfefferle, L.D. Pfefferle, Catalytically stabilized combustion, *Prog. Energy Combust. Sci.* 12 (1986) 25–41.
- [9] N.S. Kaosare, S.R. Deshmukh, D.G. Vlachos, Stability and performance of catalytic microreactors: Simulations of propane catalytic combustion on Pt, *Chem. Eng. Sci.* 63 (2008) 1098–1116.
- [10] Y.-H. Li, G.-B. Chen, F.-H. Wu, T.S. Cheng, Y.-C. Chao, Effects of catalyst segmentation with cavities on combustion enhancement of blended fuels in a micro channel, *Combust. Flame* 159 (2012) 1644–1651.
- [11] Y.-H. Li, G.-B. Chen, H.-W. Hsu, Y.-C. Chao, Enhancement of methane combustion in microchannels: Effects of catalyst segmentation and cavities, *Chem. Eng. J.* 160 (2010) 715–722.
- [12] Y.-H. Li, G.-B. Chen, T.-S. Cheng, Y.-L. Yeh, Y.-C. Chao, Combustion characteristics of a small-scale combustor with a percolated platinum emitter tube for thermophotovoltaics, *Energy* 61 (2013) 150–157.
- [13] Y.-H. Li, G.-B. Chen, Y.-S. Lien, Y.-C. Chao, Development of a high-flame-luminosity thermophotovoltaic power system, *Chem. Eng. J.* 162 (2010) 307–313.
- [14] Y.-H. Li, C.-Y. Wu, H.-Y. Li, Y.-C. Chao, Concept and combustion characteristics of the high-luminescence flame for thermophotovoltaic systems, *Proc. Combust. Inst.* 33 (2011) 3447–3454.
- [15] P.D. Ronney, Analysis of non-adiabatic heat-recirculating combustors, *Combust. Flame* 135 (2003) 421–439.
- [16] CFDRC, 2003, CFD-ACE, Huntsville, Alabama.
- [17] O. Deutschmann, R. Schmidt, F. Behrendt, J. Warnatz, Numerical modeling of catalytic ignition, *Proc. Combust. Inst.* 26 (1996) 1747–1754.
- [18] O. Deutschmann, L.I. Maier, U. Riedel, A.H. Stroemman, R.W. Dibble, Hydrogen assisted catalytic combustion of methane on platinum, *Catal. Today* 59 (2000) 141–150.
- [19] C.P. Chen, Y.C. Chao, Y.C. Wu, J.C. Lee, G.B. Chen, Development of a catalytic hydrogen micro-propulsion system, *Combust. Sci. Technol.* 178 (2006) 2039–2060.
- [20] T.S. Cheng, C.Y. Wu, C.P. Chen, Y.H. Li, Y.C. Chao, Detailed measurement and assessment of laminar hydrogen jet diffusion flames, *Combust. Flame* 146 (2006) 268–282.